A photoelectron spectroscopic study of aqueous tetrabutylammonium iodide

2007 J. Phys.: Condens. Matter 19 326101

(http://iopscience.iop.org/0953-8984/19/32/326101)

IOP PUBLISHING JOURNAL OF PHYSICS: CONDENSED MATTER

J. Phys.: Condens. Matter **19** (2007) 326101 (9pp) doi:10.1088/0953-8984/19/32/326101

A photoelectron spectroscopic study of aqueous tetrabutylammonium iodide

H Bergersen[1], R R T Marinho[1], W Pokapanich[1], A Lindblad[1], O Björneholm[1], L J Sæthre[2] and G Öhrwall[1]

[1] Department of Physics, Uppsala University, Box 530, SE-751 21 Uppsala, Sweden
[2] Department of Chemistry, University of Bergen, NO-5007 Bergen, Norway

E-mail: henrik.bergersen@fysik.uu.se

Received 21 March 2007, in final form 15 June 2007
Published 13 July 2007
Online at stacks.iop.org/JPhysCM/19/326101

Abstract

Photoelectron spectra of tetrabutylammonium iodide (TBAI) dissolved in water have been recorded using a novel experimental set-up, which enables photoelectron spectroscopy of volatile liquids. The set-up is described in detail. Ionization energies are reported for I^- 5p, I^- 4d, C 1s and N 1s. The C 1s spectrum shows evidence of inelastic scattering of the photoelectrons, that differs from the case of TBAI in formamide.

(Some figures in this article are in colour only in the electronic version)

1. Introduction

For several decades, x-ray photoelectron spectroscopy (XPS) has been used extensively to investigate the geometric and electronic structure of molecules, clusters and solids [1, 2]. However, the application of this method to liquids is non-trivial, since the high vapour pressure of many liquids prohibits the photoelectrons from reaching the spectrometer. Furthermore, it is difficult to handle a liquid volume exposed to vacuum, since evaporation tends to either freeze or deplete the sample.

One way of overcoming these problems is to combine a differentially pumped enclosure of the sample and a small, renewable, volume of liquid. In early experimental set-ups the latter was achieved either by a millimetre-sized jet [3] or by a rotating metal disc submerged in a cup of liquid [4]. As the disc rotates, the liquid will cover the metal surface, and the film can be ionized. Liquid flowing in a shallow groove has also been used [5]. Unfortunately, these methods only allowed studies of liquids with low vapour pressure. In the only published studies of liquid water, large amounts of salt were added, which allowed substantial cooling, to suppress the vapour pressure [6, 7].

Important improvements were made by Faubel and co-workers, who used a liquid jet set-up, where the size of the jet was reduced to the micrometre-size range [8]. Such a small source

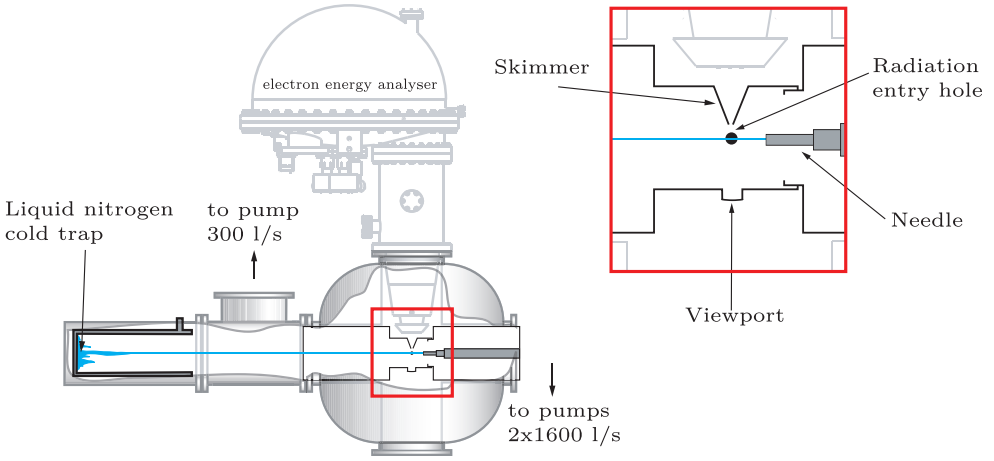

Figure 1. The experimental set-up. The enlargement shows the central part, where the ionization takes place.

enabled them to record the first photoelectron spectrum of pure liquid water [9]. However, using HeI radiation, only the outer valence region could be probed. This set-up has been adapted to synchrotron radiation by Winter and co-workers. They have published several papers on the full valence region of liquid water and aqueous solutions [10–12]. A comprehensive overview of the field of photoemission from liquids can be found in [13].

In this contribution we study aqueous tetrabutylammonium iodide (TBAI), using a set-up similar to that of Winter and co-workers. TBAI is a salt consisting of an iodide anion, I^-, and a tetrabutylammonium cation, $(CH_3CH_2CH_2CH_2)_4N^+$. TBAI is surface active because of hydrophobic interactions between water molecules and the butyl groups [14, 15]. Surface activity is a phenomenon readily examined by photoelectron spectroscopy, and hence TBAI has been studied previously. Core-level photoelectron spectra of TBAI dissolved in formamide have been published by Siegbahn and co-workers [16, 17] and by Morgner and co-workers [5], and photoelectron spectra of aqueous TBAI have been published by Winter *et al*, but only of the outer electronic levels [11].

TBAI is also important for charge transport in dye-sensitized solar cells [18–20], and in research related to this knowledge of the electronic levels in aqueous TBAI provides important reference data. In this contribution we present photoelectron spectra of aqueous TBAI, with emphasis on the previously unpublished core levels.

2. Experimental set-up

The experimental set-up is based on a differentially pumped micrometre-sized liquid jet, depicted in figure 1.

The jet is produced inside a differential pumping stage by pushing liquid at high pressure (around 50 bar) through a glass needle with a diameter of 10 μm (Micro Jet Components, part number 200.021). The needle is connected to a liquid vessel, which is pressurized by a N_2 gas bottle. The jet produced is typically somewhat smaller than the diameter of the needle [8]. The velocity of the jet can be estimated by the Bernoulli equation:

$$v = \sqrt{\frac{2P}{\rho}} \tag{1}$$

where v is the flow velocity, P is the backing pressure and ρ is the density of the liquid. For water, a backing pressure of 50 bar yields a flow velocity of around 70 m s^{-1}. The jet breaks up into droplets at a distance L from the needle that can be estimated using the relation [21, 22]

$$L = 12v\left[\sqrt{\frac{\rho d^3}{\sigma}} + \frac{3\eta d}{\sigma}\right] \tag{2}$$

where σ is the surface tension, η is the viscosity, and d is the diameter. For 50 bar backing pressure and a 10 μm nozzle diameter, this distance is 5 mm for water.

The needle is mounted on a VG Omniax manipulator with 400 mm travel. The position of the needle along the jet flow direction can be varied to probe the jet at different distances from the jet formation. In this project we used a distance from the needle to the ionization point of around 5 mm. The positions in the other directions were optimized for liquid signal strength.

The liquid jet is ionized by synchrotron radiation. The inner part of the differential pumping stage has a 1 mm hole at a right angle with respect to the jet, where the synchrotron radiation enters, and an exchangeable skimmer, at present with a 0.5 mm opening diameter, at a right angle with respect to both the liquid jet and the synchrotron radiation through which the photoelectrons are transmitted. The distance from the jet to the skimmer is 2 mm. After ionization the jet is collected by a liquid-nitrogen cold trap.

The differential pumping stage is pumped by two 1600 l s^{-1} turbo-molecular pumps upstream of the ionization point and one 300 l s^{-1} turbo-molecular pump downstream. These pumps are equipped with cold traps between the turbo pumps and the fore pumps. Typical working pressures are in the 10^{-5} mbar range in the differential pumping stage and in the 10^{-6} mbar range in the analyser. Note that the former pressure is measured far away from the jet. Close to the surface of the jet the pressure will be equal to the vapour pressure. The continuous evaporation of molecules from the jet will gradually lower the temperature of the jet. The temperature at a given point is difficult to estimate, but measuring upstream of the point where the jet breaks up into drops, the jet is still liquid, i.e. the temperature is above the melting point.

Commercially obtained TBAI was mixed with deionized water to obtain a concentration of 0.04 m (molal = mol/kg solvent). All spectra were recorded at beamline I411 at MAX-Lab in Lund, Sweden [23], using a Scienta R-4000 electron analyser. The whole set-up, including spectrometer and differential pumping stage, can be rotated around the photon beam, allowing angle-resolved measurements. In the present experiments, the spectrometer was mounted at 90° with respect to the polarization plane of the synchrotron radiation. For the overview spectrum (figure 2) the photon energy was 103 eV and the experimental resolution, due to the finite bandwidth of the radiation and spectrometer, was 60 meV. For the I^- 5p spectrum the photon energy was 60.5 eV and the resolution was 60 meV. The C 1s spectra were recorded for three different photon energies, 330, 356 and 440 eV. The experimental resolution was 180 meV in the first two cases and 240 meV in the last case. The N 1s spectrum was recorded using a photon energy of 440 eV, and the experimental resolution was 240 meV.

The experimental spectra were fitted by a least-squares technique to the lineshape given by equation (12) in [24] to account for the finite lifetime of the core–hole and the interaction between the photoelectron and the Auger electron emitted in the deexcitation of the core–hole state (post-collision interaction). Finally, the lineshape was convoluted by a Gaussian distribution to account for vibrational excitations, variations in the chemical environment between different molecules in the liquid, and the finite experimental resolution. The fitting parameters were in all cases the vertical energies and Gaussian widths of each peak as well as a linear background. All spectra have been calibrated against the I^- 4d level, which in turn is calibrated against the X state of gas-phase water [25]. Although the comparison of gas-phase

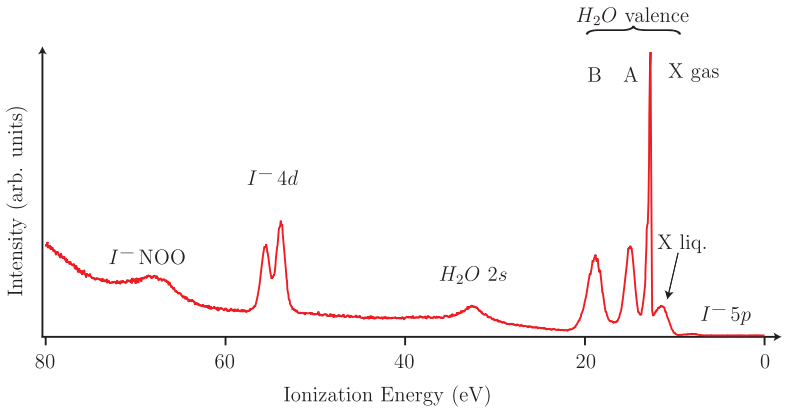

Figure 2. The photoelectron spectrum of aqueous TBAI obtained with 103 eV photon energy. The spectrum shows the I^- 4d and 5p photolines and NOO Auger lines, as well as several lines originating from both liquid and evaporated water.

and liquid energies may be complicated by possible photoelectron charging of the liquid beam, we estimate the uncertainties in the given energies to be less than 0.2 eV.

3. Computational details

For C 1s ionization, depicted in figure 4, the relative ionization potentials for the four inequivalent carbon atoms in the free TBA^+ ion (or for all 16 carbons in the case of the crystalline structure [26]) have been calculated in the following way. For the neutral state we have used Gaussian 03 [27] with the B3LYP method to calculate the optimized geometry. Vertical relative ionization energies have been calculated by comparing the total energy of the different core-ionized species in the ground-state geometry. In all calculations atom-centred Gaussian-type functions contracted to triple-zeta quality and augmented by polarization functions were used [28]. The core of the ionized carbon atom was represented by the effective core potential (ECP) of Stevens *et al* [29], scaled to account for only one electron in the 1s shell [30]. Calculations were also performed using a polarizable dielectric continuum (PCM) model to simulate the solvation [31]. In that case a dielectric constant of 1.776 was used in the ionized state, to model the electronic part of the polarization, since the core–hole lifetime is too short for any nuclear relaxation to occur. Since the calculations are based on the use of an effective core potential rather than an explicit core–hole, absolute energies cannot be obtained.

4. Results and discussion

4.1. Valence and shallow core level region

Figure 2 shows the photoelectron spectrum of aqueous TBAI obtained with a photon energy of 103 eV. A similar spectrum is presented in [12], and it is shown here for completeness. The spectrum shows several I^- lines from the salt, as well as lines originating from water, both liquid and evaporated. The valence signal from the TBA^+ ion is too weak to be detected. The liquid signal is broader and shifted to lower ionization energy than its gas-phase counterpart. This can most easily be seen in the X state, where the gas and liquid lines are well separated. The shift is dominated by the electrostatic screening of the final state, and the broadening

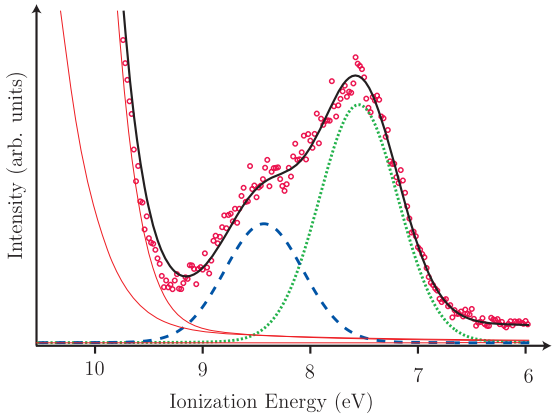

Figure 3. The I^- 5p photoelectron spectrum of aqueous TBAI obtained with 60.5 eV photon energy. Circles are experimental data points. The dashed line shows the $5p_{1/2}$ and the dotted line shows the $5p_{3/2}$ component. The thin solid lines represent the X state of liquid water. The thicker solid line shows the sum of the lineshapes.

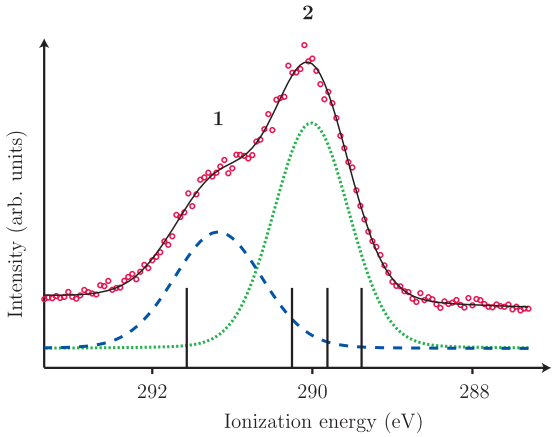

Figure 4. The C 1s photoelectron spectrum of aqueous TBAI obtained with 330 eV photon energy. Circles are experimental data points. The dashed line shows the peak corresponding to the carbons bonded to the central nitrogen atom (peak **1**). The dotted line shows the peak corresponding to ionization of the butane-like carbons (peak **2**). The solid line shows the sum of the lineshapes. The bars represent calculated ionization energies for the four inequivalent carbons. The bars have been shifted to overlap with the experimental features.

results from the distribution of ionization energies (generally due to both initial and final state effects) between different sites in the liquid. Compared to the corresponding spectra of [12], our spectrum shows more gas-phase signal. This is a consequence of the larger radiation spot size and the larger spectrometer skimmer of our set-up.

4.2. I^- 5p region

Figure 3 shows the I^- 5p photoelectron spectrum of aqueous TBAI, together with Gaussian profiles representing the two spin–orbit components obtained from a least-squares fit to the experiment. The large structure at higher ionization energy is the X state of liquid water. That

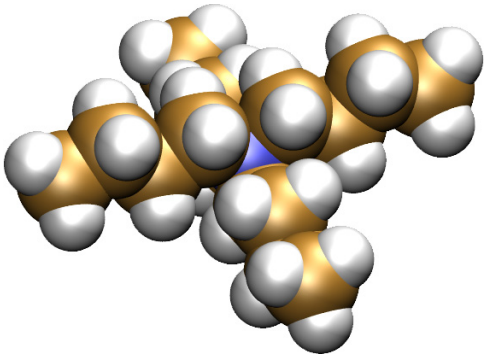

Figure 5. The structure of the free TBA^+ ion as obtained from first-principles calculations.

peak has been fitted by an ad hoc lineshape consisting of two Gaussian profiles. The width of the I 5p peaks is 0.9 eV. The spin–orbit splitting is 0.9 eV, smaller than in Xe 5p (1.3 eV [32]), which has the same electronic configuration but a larger nuclear charge.

4.3. C 1s region

The C 1s photoelectron spectrum of aqueous TBAI is shown in figure 4, together with calculated ionization energies for the four inequivalent carbons of the TBA^+ ion. The spectrum exhibits a peak at lower ionization energy (peak **2**), and a shoulder at higher ionization energy (peak **1**). The widths of the peaks are 1.2 eV and 1.0 eV for peaks **1** and **2** respectively, and the separation between them is 1.2 eV. The calculated ionization energy is highest for the carbon bonded to nitrogen, and continuously lower for carbons farther out in the butyl chain (see figure 5). Since the calculation only provides relative ionization energies, the overall position of the bars in figure 4 is arbitrary, and has been chosen to overlap with the experimental features. By comparing the calculated energies to the experimental spectrum we find that peak **1** is due to ionization of the carbon which is bonded to nitrogen, and peak **2** is due to ionization of the other carbons. The same assignment has also been found for TBAI in formamide [17]. However, it is evident that the calculation, which is performed for the free ion, overestimates the chemical shift between the carbons. To address this we have performed calculations also for the molecule in a polarizable dielectric continuum (PCM), as well as for the gas-phase molecule in the molecular geometry found for crystalline TBAI [26]. These calculations show that the difference in relative ionization energies between these three models is only a few meV. From the experimental data we conclude that the shift between the carbons not bonded to nitrogen is very small, in agreement with what has been seen for TBAI in formamide [17]. We expect the discrepancy between calculations and experiments to be due to the interaction between the molecule and the solvent, and that the PCM is too crude a model to resolve this.

Unlike the spectra of [17], the peaks in our spectrum do not show the intensity ratio of three to one that is expected from stoichiometry. Any attempt to constrain the ratios to the stoichiometric ratios results in a unacceptable fit of the spectra. We attribute this discrepancy to inelastic scattering of the photoelectrons, meaning that, on average, the carbon atoms closest to the nitrogen atom are closer to the surface than the other carbons (see figure 5). This would then imply that the ion is oriented with some butyl groups sticking into the liquid. This is supported by Molecular Dynamics simulations reported in [12], where the butyl groups of TBA^+ are found either along the surface, or slightly sticking into the liquid. The calculations show that

Table 1. Relative intensities of the peaks observed in the C 1s spectra of aqueous TBAI. I_1 and I_2 correspond to peaks **1** and **2** of figure 4, respectively.

Photon energy (eV)	Kinetic energy (eV)	Conc. (m)	Rel. intensity (I_2/I_1)
330	40	0.04	1.66
356	65	0.04	2.06
356	65	0.02	2.38
440	150	0.04	2.22

the tendency of the butyl arms to stick into the liquid is enhanced for higher concentrations, compared to sub-monolayer concentrations. To probe this, we have recorded spectra for 0.02 m TBAI at 356 eV photon energy. 0.02 m has been shown by Winter and co-workers to be close to one monolayer coverage [12]. In this case the ratio of peak **2** to peak **1** is 2.38, compared to 2.06 for 0.04 m TBAI, consistent with increased tendency for butyl groups to point inwards in the latter case.

The inelastic scattering is expected to depend on the kinetic energy of the photoelectrons, to have a maximum at 10–100 eV kinetic energy, and to decrease with increasing kinetic energy [33]. The spectra of [17] were recorded using Al Kα radiation with a photon energy of 1487 eV, giving the photoelectrons almost 1200 eV kinetic energy, whereas our spectrum was recorded using a photon energy of 330 eV, allowing around 40 eV kinetic energy for the photoelectrons. Indeed, spectra recorded using higher photon energy show an increasing ratio of peak intensities; see table 1.

By using an assumption about the structure of the TBA^+ ions on the surface, the observed relative intensity of the peaks in the C 1s spectra can be used to estimate the effective attenuation lengths for the different kinetic energies. The standard method to do this is to assume an exponential signal attenuation as the photoelectron travels towards the surface of the sample. However, in this case, all assumptions about the structure of the molecules at the surface leads to effective attenuation lengths smaller than the size of the molecules, meaning that an exponential attenuation is not a useful model.

XPS of TBAI in formamide has also been studied in [5] using synchrotron radiation. The authors present C 1s data recorded using 380 eV photon energy, giving the photoelectrons around 90 eV kinetic energy. It is interesting to note that, in that case, the relative intensity of the peaks is much closer to the stoichiometric ratio than what we see for both 65 and 150 eV kinetic energy. We expect the effective attenuation to be monotonic with respect to kinetic energy, and hence the inconsistency between our data and the spectrum of [5] suggests either that the effective attenuation length is different for formamide and water, or that the orientation of the TBA^+ ion on the surface is different for the two solvents.

4.4. N 1s

The N 1s XPS spectrum is shown in figure 6. The spectrum shows a single peak, corresponding to ionization of the central nitrogen atom. The vertical energy is 407.4 eV, and the width is close to 1 eV, similar to the widths seen for the other core levels.

To summarize, we give the vertical energies and Gaussian widths of all investigated electronic levels in table 2.

5. Conclusions

Photoelectron spectra of aqueous tetrabutylammonium (TBAI) have been recorded. The spectra are consistent with previously published spectra of the valence region of aqueous TBAI

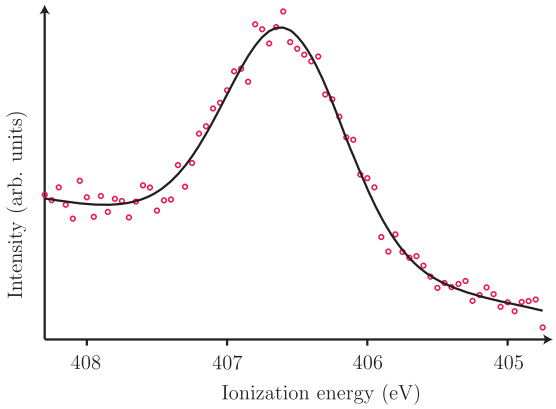

Figure 6. The N 1s photoelectron spectrum of aqueous TBAI obtained with 440 eV photon energy. A constant background has been subtracted.

Table 2. Vertical ionization energies and Gaussian widths obtained from the least-squares fit. Values given for TBA^+ C 1s correspond to peaks **1** and **2** respectively.

Electronic level	Vertical ionization energy (eV)	Gaussian width (eV)
I^- $5p_{3/2}$	7.6	0.9
I^- $5p_{1/2}$	8.4	0.9
I^- $4d_{5/2}$	53.7	1.1
I^- $4d_{3/2}$	55.4	1.1
TBA^+ C 1s		
Peak **1**	291.9	1.2
Peak **2**	290.7	1.0
TBA^+ N 1s	407.4	1.0

and TBAI in formamide, respectively. The observation of non-stoichiometric relative peak intensities in C 1s spectra is attributed to inelastic scattering of the photoelectrons, and is found to be different from the case of TBAI dissolved in formamide.

Acknowledgments

The authors would like to acknowledge fruitful discussions with Professor Knut J Børve and Dr Håkan Rensmo and help from the MAX-lab staff as well as financial support of the Knut and Alice Wallenberg foundation, Swedish Scientific Council (VR), The Swedish Foundation for strategic research (SSF), Göran Gustafsson's foundation, the Nordic Research Board, the Meltzer Foundation of the University of Bergen, CNPq-Brazil, STINT, the Royal Thai government and a computing grant from UPPMAX under project p2006027.

References

[1] Siegbahn K, Nordling C, Fahlman A, Nordberg R, Hamrin K, Hedman J, Johansson G, Bergmark T, Karlsson S-E, Lindgren I and Lindberg B 1967 *ESCA, Atomic, Molecular and Solid State Structure Studied by Means of Electron Spectroscopy* (Uppsala: Almquist and Wiksells)

[2] Hüfner S 2003 *Photoelectron Spectroscopy: Principles and Applications* (Berlin: Springer)

[3] Siegbahn H and Siegbahn K 1973 *J. Electron Spectrosc. Relat. Phenom.* **2** 319
[4] Siegbahn H, Svensson S and Lundholm M 1981 *J. Electron Spectrosc. Relat. Phenom.* **24** 205
[5] Eschen F, Heyerhoff M, Morgner H and Vogt J 1995 *J. Phys.: Condens. Matter* **7** 1961
[6] Lundholm M, Siegbahn H, Holmberg S and Arbman M 1986 *J. Electron Spectrosc. Relat. Phenom.* **40** 165
[7] Böhm R, Morgner H, Oberbrodhage J and Wulf M 1994 *Surf. Sci.* **317** 407
[8] Faubel M and Steiner B 1992 *Ber. Bunsenges. Phys. Chem.* **96** 1167
[9] Faubel M, Steiner B and Toennies J P 1997 *J. Chem. Phys.* **106** 9013
[10] Weber R, Winter B, Schmidt P M, Widdra W, Hertel I V, Dittmar M and Faubel M 2004 *J. Phys. Chem.* B **108** 4729
[11] Winter B, Weber R, Widdra W, Dittmar M, Faubel M and Hertel I V 2004 *J. Phys. Chem.* A **108** 2625
[12] Winter B, Weber R, Schmidt P M, Hertel I V, Faubel M, Vrbka L and Jungwirth P 2004 *J. Phys. Chem.* B **108** 14558
[13] Winter B and Faubel M 2006 *Chem. Rev.* **106** 1176
[14] Tamaki K 1974 *Bull. Chem. Soc. Japan* **47** 2764
[15] Tamaki K 1967 *Bull. Chem. Soc. Japan* **40** 38
[16] Holmberg S, Moberg R, Yuan Z C and Siegbahn H 1986 *J. Electron Spectrosc. Relat. Phenom.* **41** 337
[17] Holmberg S, Yuan Z C, Moberg R and Siegbahn H 1988 *J. Electron Spectrosc. Relat. Phenom.* **47** 27
[18] O'Regan B and Grätzel M 1991 *Nature* **353** 737
[19] Nazeeruddin Md K, Zakeeruddin S M, Humphry-Baker R, Jirousek M, Liska P, Vlachopoulos N, Shklover V, Fischer C-H and Grätzel M 1999 *Inorg. Chem.* **38** 6298
[20] Gregg B A, Chen S-G and Ferrere S 2003 *J. Phys. Chem.* B **107** 3019
[21] McCarthy M J and Molloy N A 1974 *Chem. Eng.* **7** 1
[22] Heinzl J and Hertz C H 1985 *Adv. Electron. Electron. Phys.* **65** 91
[23] Bässler M, Forsell J-O, Björneholm O, Feifel R, Jurvansuu M, Aksela S, Sundin S, Sorensen S L, Nyholm R, Ausmees A and Svensson S 1999 *J. Electron Spectrosc. Relat. Phenom.* **101–103** 953
[24] van der Straten P, Morgenstern R and Niehaus A 1988 *Z. Phys.* D **8** 35
[25] Karlsson L, Mattsson L, Jadrny R, Albridge R G, Pinchas S, Bergmark T and Siegbahn K 1975 *J. Chem. Phys.* **62** 4745
[26] Wang Q, Habenschuss A, Xenopoulos A and Wunderlich B 1995 *Mol. Cryst. Liq. Cryst.* **264** 115
[27] Frisch M J, Trucks G W, Schlegel H B, Scuseria G E, Robb M A, Cheeseman J R, Montgomery J A Jr, Vreven T, Kudin K N, Burant J C, Millam J M, Iyengar S S, Tomasi J, Barone V, Mennucci B, Cossi M, Scalmani G, Rega N, Petersson G A, Nakatsuji H, Hada M, Ehara M, Toyota K, Fukuda R, Hasegawa J, Ishida M, Nakajima T, Honda Y, Kitao O, Nakai H, Klene M, Li X, Knox J E, Hratchian H P, Cross J B, Adamo C, Jaramillo J, Gomperts R, Stratmann R E, Yazyev O, Austin A J, Cammi R, Pomelli C, Ochterski J W, Ayala P Y, Morokuma K, Voth G A, Salvador P, Dannenberg J J, Zakrzewski V G, Dapprich S, Daniels A D, Strain M C, Farkas O, Malick D K, Rabuck A D, Raghavachari K, Foresman J B, Ortiz J V, Cui Q, Baboul A G, Clifford S, Cioslowski J, Stefanov B B, Liu G, Liashenko A, Piskorz P, Komaromi I, Martin R L, Fox D J, Keith T, Al-Laham M A, Peng C Y, Nanayakkara A, Challacombe M, Gill P M W, Johnson B, Chen W, Wong M W, Gonzalez C and Pople J A 2004 *Gaussian 03, rev c.02* (Wallingford, CT: Gaussian)
[28] Krishnan R, Binkley J S, Seeger R and Pople J A 1980 *J. Chem. Phys.* **72** 650
[29] Stevens W J, Basch H and Krauss M 1984 *J. Chem. Phys.* **81** 6026
[30] Karlsen T and Børve K J 2000 *J. Chem. Phys.* **112** 7986
[31] Cossi M, Barone V, Cammi R and Tomasi J 1996 *Chem. Phys. Lett.* **255** 327
[32] Moore C E 1949 Atomic energy levels *Circular of the National Bureau of Standards 467* (Washington, DC: US Govt Printing Office)
[33] Powell C J, Jablonski A, Tilinin I S, Tanuma S and Penn D R 1999 *J. Electron Spectrosc. Relat. Phenom.* **98/99** 1